hydrate stage of weddellite has been variously reported during the last 30 years. Frey-Wyssling (*2*), Klasens, Perdok, and Terpstra (*3*), and Pobeguin (*4*) found a formula weight of three molecules of water per molecule of salt. However, Honegger's measurements (*5*) indicate 2.5 molecules of water as the hydrate composition, while Bannister and Hey (*1*) and Gasser, Brauner, and Preisinger (*6*) reported that the tetragonal crystal of calcium oxalate is a dihydrate. Philipsborn (*7*) determined that weddellite is a dihydrate which can take up a maximum of one-half mole of zeolitic water per mole of salt. Most recently, Walter-Lévy and Laniepce (*8*) measured values of 2.27 to 2.32 for the ratio H_2O:Ca and accepted the figure 2.25 for the hydrate composition.

A presumptive specimen of weddellite, in the form of a kidney calculus of macroscopically individualized tetragonal crystals, was subjected to x-ray analysis. The x-ray diffraction diagram of the ground crystal powder was that of typical weddellite (*5*). Intensity data (720 independent reflections) were obtained with CuKα radiation from a single crystal, 0.25 by 0.1 mm, by photographic methods with the Weissnberg technique, the crystal being rotated about the [100] axis.

The space group is I4/m. (The structure could not be refined in the space groups I$\bar{4}$ and I4). The unit cell has the dimensions, $a = 12.30 \pm 0.02$ Å, $c = 7.34 \pm 0.02$ Å. Density by flotation is 2.00 g/ml, so that $Z = 8$.

The positions of the salt atoms and of the two water-oxygen atoms of a dihydrate were derived from the three-dimensional Patterson function. With these atoms, refinement of all the data by least squares reduced

$$R = \Sigma \,||\, F_{\text{obs}} \,|-|\, F_{\text{calc}} \,||\, / \,\Sigma \,|\, F_{\text{obs}} \,|$$

to 0.179. At this stage, three-dimensional Fourier synthesis of F_{obs}-F_{calc} and also F_{obs} alone showed an unaccounted-for peak density of about 2 to 3 electrons per cubic angstrom on the 4-fold axis, occupying the center of the only relatively open position within the unit cell. This peak was taken to represent the presence of a disordered water molecule at that site (a water molecule here would give the maximum hydrate condition of the salt as 2.5 H_2O). Placement of an oxygen atom in the indicated position improved *R* to 0.174, but the atom had an unusually large thermal parameter (17 Å^2). It appeared either that the atom was incorrectly placed (that the water molecule does not lie exactly on the 4-fold axis) or that—if the cell is zeolitic—there was not the equivalent of a full water molecule in this position. The first alternative was ruled out by calculation. On the basis of the second alternative, with 0.4 of an oxygen atom on the 4-fold axis (that is, corresponding to the formula $CaC_2O_4 \cdot 2.2\ H_2O$), *R* was lowered to 0.171, and the thermal parameter of the water oxygen was reduced to a more reasonable 5.7 Å^2. When a smaller fraction (0.2) of an atom was used, the thermal parameter became negative. The crystallographically determined water composition of this particular weddellite crystal thus is in accord with the measured density, which gives 2.17 H_2O per CaC_2O_4 moiety. Further least squares refinement, on the basis of assigning the unobserved intensities one-half the value of the smallest observed intensity, rather than zero, lowered *R* to 0.141. Treatment of the calcium ion as having anisotropic thermal movement gave only a slight improvement, with a final *R* value of 0.138. Without the unobserved intensities, *R* is 0.130.

Table 1. Atomic coordinates and thermal parameters in weddellite ($CaC_2O_4 \cdot 2.2\ H_2O$).

Atom	*x*	*y*	*z*	*B*, Å^2
Ca	0.200	0.300	0	(0.4)*
O (1)	.356	.246	0.181	1.0
O (2)	.537	.236	.180	2.2
O (w1)	.144	.114		1.8
O (w2)	.020	.386		2.6
O (w3)			.291	5.7
C	.445	.242	.105	0.9

* Isotropic *B* equivalent to average of anisotropic temperature factor.

Atomic coordinates and thermal parameters are given in Table 1. The calcium atom is coordinated with eight oxygen atoms (two water-oxygen atoms and six oxalate-oxygen atoms), which are roughly arranged in the form of a cubic anti-prism, with an average C—O distance of 2.45 Å. The oxalate ion is planar, and the C—C bond is bisected by a symmetry plane. Therefore the oxalate ion has at least the symmetry *2mm*, the bond lengths being C(1)—C(2), 1.55 ± 0.02 Å; C(1)—O(1), 1.23 ± 0.01 Å; C(1)—O(2), 1.26 ± 0.01 Å. The bond angles are C(2)—C(1)—O(1), 117.0 ± 0.5°, C(2)—C(1)—O(2), 115.9 ± 0.5°; O(1)—C(1)—O(3), 127.1 ± 0.8°. Because the differences between corresponding bond lengths and bond angles do not have statistical significance, it is conceivable that the symmetry of the oxalate ion here may be *mmm*.

Hydrogen atoms are not detectable with these data. Hydrogen bonds are assigned on the basis of appropriate lengths and angles to those O—O distances which appear to interconnect primitive cells: 2 [O(w1)—O(1)′], O(w2)—O(2)′, O(w2)—O(w2)′, with the respective bond distances, 2.91 ± 0.01 Å, 2.87 ± 0.01 Å, 2.84 ± 0.02 Å. The water molecule O(w3) is 3.06 ± 0.12 Å from the water oxygen O(w3)′, 3.11 ± 0.04 Å from the water oxygen O(w1), and 3.29 ± 0.01 Å from the oxalate oxygen O(2)′.

CLARENCE STERLING

Department of Food Science and Technology, University of California, Davis

References and Notes

1. F. A. Bannister, *Discovery Repts.* **13**, 60 (1936).
2. A. Frey-Wyssling, *Die Stoffausscheidung der Höheren Pflanzen* (Springer, Berlin, 1935), p. 151.
3. H. A. Klasens, W. G. Perdok, P. Terpstra, *Z. Krist. (A)* **96**, 227 (1937).
4. T. Pobeguin, *Ann. Sci. Nat. Botan. XI.* **4**, 1 (1943).
5. R. Honegger, "Das Polyhydrat des Kalzium-Oxalates," dissertation, Univ. of Zürich (1952).
6. G. Gasser, K. Brauner, A. Preisinger, *Z. Urol.* **49**, 148 (1956).
7. H. V. Philipsborn, *Protoplasma* **41**, 415 (1952).
8. L. Walter-Lévy, J. Laniepce, *Compt. Rend.* **254**, 1073 (1962).
9. Work supported by a J. S. Guggenheim Memorial Foundation fellowship. Part of it was done at the Mineralogical Institute of the University of Vienna. I thank Prof. A. Preisinger for the weddellite specimen and for use of Institute facilities. A more detailed report will appear elsewhere.

2 September 1964

High-Pressure Polymorphs in the Silver Iodide Phase Diagram

Abstract. *A good x-ray diffraction pattern has been obtained for the new phase of silver iodide stable in the vicinity of 3 kilobars at room temperature. A stability diagram of the six phases of silver iodide is presented to show the probable position of the narrow stability field of this phase. The x-ray diffraction data indicate that the cell symmetry of the new phase is probably orthorhombic.*

It now appears that silver iodide can exist in at least six polymorphic modifications. At room temperature and atmospheric pressure, that the stable form is hexagonal wurtzite type (II, Fig. 1) is evident from the careful work of

Burley (*1*). This phase is readily converted, by grinding in a mortar or by pressing, to a metastable sphalerite-type form (II′), which at temperatures above 80°C (and below 146°C) is observed to transform spontaneously and irreversibly to the hexagonal wurtzite-type modification. Moreover, it seems likely that below 80°C the wurtzite-type form is the stable one, although at these low temperatures the sphalerite-type form persists indefinitely. For this reason Majundar and Roy (*2*) conclude that a true stability region of phase II′ does not exist. Here is a case in which not only the densities but also the lattice energies (*3*) are nearly the same at room temperature. Apparently the free energies are also so similar that it is academic to label one form as the stable one, and the other metastable.

Above 146°C phase II inverts to a cubic, disordered body-centered form (*4*), and above about 3-kb pressure Bridgman (*5*) found a cubic form now known to be halite type (*6*). At 97 kb, Riggleman and Drickamer (*7*) observed a new phase by means of high-pressure electrical resistance studies; Bassett and Takahashi (*8*) observed a similar phase change at 110 kb by x-ray and optical methods and proposed that the new phase (V, Fig. 1) has a CsCl-type structure. Bassett and Takahashi also confirmed the existence of another new phase (IV), first found by Van Valkenburg (*9*), which at room temperature exists in a very narrow stability field near 3 kb.

Phases I, II, and III meet in a triple point at 2.7 kb and 100°C (*5*). Bassett and Takahashi (*8*) report another triple point at lower temperature, and at approximately the same pressure, between phases II, III, and IV.

The pressure interval for the stable existence of the new form (IV) of AgI can be estimated from the photograph in the report by Van Valkenburg [(*9*) and Fig. 1]. In the photograph the width of the ring Δr pertaining to the new phase is about 0.15 at $r = 0.63$, where r is the fractional radius of the anvil. By considering various types of pressure gradients across the anvil, it appears that the range of pressure for the stable existence of phase IV can be only a few tenths of a kilobar at room temperature.

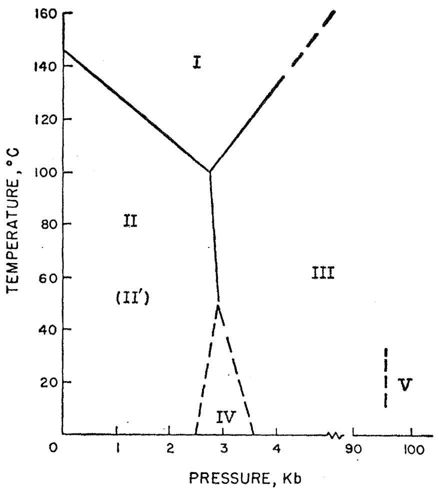

Fig. 1. Phase diagram of silver iodide. The dashed boundaries give the approximate positions of the stability fields of phases IV and V.

Table 1. X-ray diffraction data for AgI-phase IV at 25°C and 3 ± 0.5 kb.

d_{obs} Å	Form						I/I_0 §
	Hexagonal *		Tetragonal †		Orthorhombic ‡		
	hkl	d_{calc} Å	*hkl*	d_{calc} Å	*hkl*	d_{calc} Å	
6.04	101	6.00	101	6.01	011	6.10	5
3.97	200	3.98	201	3.97	012	4.00	4
3.66	201	3.65	102	3.66	112	3.68	55
2.86	211	2.86	212	2.86	013	2.87	64
2.50	212	2.51	222	2.51	131	2.51	17
2.30	220	2.30	203	2.30	004	2.30	94
2.20	310	2.21	401	2.20	014 303	2.21 2.19	100
1.995	400	1.992	004	1.995	140	1.991	40
1.949	401	1.945	104	1.949	141	1.946	40
1.829	320 223	1.828 1.827	204 500	1.829 1.828	142	1.828	20
1.624	412	1.622	423	1.621	050	1.630	28
1.503	502 420	1.503 1.506	404 610 205	1.503 1.503 1.506	135	1.504	26
1.409	503 206	1.408 1.407	612 541	1.407 1.405	434	1.405	16
1.380	414	1.377	443	1.381	540 352	1.380 1.379	5
1.304	504 306	1.301 1.308	116 700 613 405	1.303 1.306 1.308 1.308	326 062 260	1.304 1.303 1.305	23
1.258	432 226	1.258 1.258	543 425 444	1.258 1.258 1.256	543 721 262	1.258 1.260 1.255	7
1.246	316 117	1.243 1.241	702 721	1.241 1.240	360 063 525	1.246 1.243 1.250	19

* $v(H) = 0.1413$ cm³/g ($Z = 12$); † $v(T) = 0.1426$ cm³/g ($Z = 12$); ‡ $v(O) = 0.1518$ cm³/g ($Z = 12$); § Ratios of integrated intensitics.

Van Valkenburg's optical study of this phase showed that it was not isometric. The beryllium vessel technique (*10*) was considered ideal for the study of the high-pressure x-ray diffraction patterns of this phase. Because of the demonstrated narrow pressure range of stability of the form at room temperature, the sample was packed in cornstarch, and this procedure was highly successful in creating near hydrostatic conditions in the vessel. An estimated 75 percent conversion to the new phase was accomplished with this technique. However, in all experiments at least one of the two adjacent phases II′ or III was also present, and in most instances, both were present. From this fact, and because heating to 50°C of a mixture of II′, III, and IV at about 3 kb caused the peaks from phase IV to disappear and the peaks from phases II′ and III to increase slightly in intensity, the triple point II-III-IV is probably lower than the 85°C reported by Bassett and Takahashi (*8*). It is possibly no higher than 50°C and may be even closer to room temperature. The boundaries of phase IV in Fig. 1 are dashed to show only the approximate position of its stability field.

With the use of the beryllium pressure vessel and an x-ray fluid-pressure cell (*11*), several excellent x-ray diffraction patterns of phase IV have been obtained from which 17 reproducible peaks can be identified. The peaks were first indexed according to a hexagonal cell (H) that appears to be related to the wurtzite-type (II) cell according to the relations

$$a_H \cong 2a_{II},$$
$$(h00)_{II} = \tfrac{1}{2}(h00)_H,$$
$$(hk0)_{II} = \tfrac{1}{2}(hk0)_H$$

where a_{II} = 4.59 Å, c_{II} = 7.51 Å, a_H = 9.20 Å, and c_H = 9.02 Å. There does not appear to be any relation between the c-directions of the two structures. Constants for two other cells, tetragonal (T) and orthorhombic (O), can be derived from the hexagonal one according to the relations

$$a_T \cong (a_H + c_H)/2 \qquad a_T = 9.14\ \text{Å}$$
$$c_T = (\sqrt{3}/2)a_H \qquad c_T = 7.98\ \text{Å}$$

and

$$a_O = 1.055\ a_T \qquad a_O = 9.37\ \text{Å}$$
$$b_O = 0.892\ a_T \qquad b_O = 8.15\ \text{Å}$$
$$c_O = a_H \qquad c_O = 9.20\ \text{Å}$$

Indexing of the three cells can be accomplished with nearly the same degree of fit, and therefore the indices for all three are presented in Table 1. The measured specific volume of phase II at 1 atm is 0.1759 cm^3/g, and for phase III at 3 kb, 0.1431 cm^3/g. In view of the specific volume of these cells with Z equal to 12 molecules per cell, as presented in Table 1, the orthorhombic cell appears to be the most acceptable. For the tetragonal cell, Z equal to 10 gives a specific volume of 0.1711 cm^3/g, a possibility that as yet cannot be ruled out.

It is our suggestion that any further attempt to obtain x-ray diffraction data for this phase should be carried out in an apparatus employing perfectly hydrostatic pressures. We have made several unsuccessful attempts to obtain the phase IV diffraction pattern using the beryllium Bridgman anvil apparatus (*12*, Fig. 1*A*). The narrow range of stability of the form combined with the pressure gradient of such devices results in such a small quantity converted [approximately 15 percent in the anvil shown in Fig. 1 of the Van Valkenburg paper (*9*)] that it is difficult to obtain definitive x-ray diffraction patterns. It is evident, however, that pressure gradients in the anvil device can be considerably reduced by cycling the pressure up and down until there is no more extrusion of the sample (*9*, p. 97).

BRIANT L. DAVIS*
LEASON H. ADAMS

Institute of Geophysics and Planetary Physics, University of California, Los Angeles

References and Notes

1. G. Burley, *J. Phys. Chem.* **68**, 1111 (1964).
2. A. J. Majumdar and R. Roy, *ibid.* **63**, 1858 (1959).
3. G. Burley, *Am. Mineral.* **48**, 1266, 1273 (1963); M. L. Huggins, in *Phase Transformations in Solids*, R. Smoluchowski, Ed. (Wiley, New York, 1951), p. 246.
4. L. W. Strock, *Z. Physik. Chem.* **25**, 441 (1934).
5. P. W. Bridgman, *Proc. Am. Acad. Arts Sci.* **51**, 55 (1915).
6. R. B. Jacobs, *Phys. Rev.* **54**, 468 (1938).
7. B. M. Riggleman and H. G. Drickamer, *J. Chem. Phys.* **38**, 2721 (1963).
8. W. A. Bassett and T. Takahashi, *Am. Geophys. Union Trans.* **45**, 121 (1964).
9. A. Van Valkenburg, *J. Res. Natl. Bur. Stds. A* **68**, 97 (1964).
10. B. L. Davis and L. H. Adams, *J. Phys. Chem. Solids* **25**, 379 (1964).
11. L. H. Adams and B. L. Davis, in preparation.
12. B. L. Davis and L. H. Adams, *Z. Krist.* **117**, 399 (1962).
13. Publication No. 388, Institute of Geophysics and Planetary Physics, University of California, Los Angeles. Supported by grants from the National Science Foundation.

* Present address: Department of Geology and Geological Engineering, South Dakota School of Mines and Technology, Rapid City.

13 July 1964

Effect of Traces of Large Molecules Containing Nitrogen on Hydrogen Overvoltage

Abstract. *Organic amines, present in very small concentrations (below* 10^{-6}M) *in* 0.1N H_2SO_4, *cause a significant increase in hydrogen overvoltage, the effect being stronger the higher the molecular weight. The increase could be accounted for by the usual site-blockage concept. In the case of egg albumin, a drastic increase of over 300 mv was observed at 12.5 ma/cm^2 for a concentration of only 0.01 part per million. A new mechanism is proposed in which the dielectric constant and hydrogen-ion activity are believed to be depressed in a region twice as thick as the usual transition region.*

Hydrogen overvoltage is defined as the difference between the potential of an electrode at which hydrogen is being evolved at a given current density and the potential of a standard (reversible) hydrogen electrode in the same solution (*1*). While the current flows between the working hydrogen electrode and an anode elsewhere in the solution, the overvoltage is measured between the working hydrogen electrode and a standard reference electrode by means of a Luggin capillary at the surface of the working electrode.

The magnitude of the hydrogen overvoltage in acid solutions has been attributed largely to the kinetics of transfer, discharge, and recombination reactions involving the cathode and the so-called "Stern" double layer (*2*) which acts like a capacitor. Beyond the Stern double layer is a diffusion-controlled polarization layer which is diluted during electrolysis. Both the Stern and polarization layers introduce resistance giving rise to an "IR drop" voltage. Generally, for small and moderate current densities, and under agitation, it appears justifiable to neglect the IR drop (*3*), as is implied when the measured overvoltage is calculated from the electrode kinetics. In the presence of impurities or contaminants, hydrogen evolution usually occurs at a higher overvoltage than it does when the surface is scrupulously clean (*3*, p. 131). This effect is known as "poisoning" (*4*). While such poisoning effects have been known for a long time (*1*, *5*), little work appears to have been done in measuring the effect of trace amounts (10^{-6} to $10^{-8}M$) of organic compounds with large molecules in aqueous solution. Yet such results would have both practical and theoretical implications. We have found that amines of high molecular weight, at these low concentrations, can significantly affect the overvoltage at a lightly platinized electrode, and that egg albumin at 0.01 ppm increases it drastically. We believe that these results shed new light on the mechanism of interaction of organic compounds with a hydrogen electrode, and suggest a possible explanation for this effect.

Our studies were made in both a large (500 ml) unstirred all-glass cell and in a small (15 ml) flowing cell. The flowing cell was also constructed entirely of glass, with adjustable cathode-to-reference spacing and provision to vary the flow rate from 0 to 10 ml/sec. Both cells were operated under a hydrogen atmosphere with 0.1N H_2SO_4 as the standard electrolyte; data were recorded on a Sanborn model 150 recorder.

In Fig. 1 the overvoltage is plotted as a function of current density for a number of organic amines and quaternary ammonium compounds. The shaded area A indicates the reproducibility of control runs with no added organic compounds for both types of cell. Tetramethylammonium bromide (TMAB) (cation equivalent weight 72) and ethanolamine (equivalent weight 61) did not produce an increase in hydrogen overvoltage which fell outside the